Research Square

Preprints are preliminary reports that have not undergone peer review.
They should not be considered conclusive, used to inform clinical practice,
or referenced by the media as validated information.

Chronic high-phosphate exposure impairs intestinal health in juvenile turbot (Scophthalmus maximus) reared in recirculating aquaculture systems

Jiale Zhou
Ocean University of China
Lele Wu
Ocean University of China
Xin Li
Ocean University of China
Xiangyu Zhang
Ocean University of China
Ting Qi
Ocean University of China
Xian Li
lixian@ouc.edu.cn

Ocean University of China

Research Article

Keywords: Digestive enzyme activity, Oxidative stress, Intestinal microbiota

Posted Date: November 23rd, 2026

DOI: https://doi.org/10.21203/rs.3.rs-11519393/v1

License: This work is licensed under a Creative Commons Attribution 4.0 International License.
Read Full License

Additional Declarations: No competing interests reported.

Chronic high-phosphate exposure impairs intestinal health in juvenile turbot (*Scophthalmus maximus*) reared in recirculating aquaculture systems

Jiale Zhou[a#], Lele Wu[a#], Xin Li[a], Xiangyu Zhang[a], Ting Qi[a], Xian Li[a, b*]

[a] Key Laboratory of Mariculture (Ministry of Education), Fisheries College, Ocean University of China, Qingdao 266001, PR China

[b] Shandong Key Laboratory of Green Mariculture and Smart Fisheries, Qingdao 266001, PR China

[#]These authors contributed equally to this work.

*Correspondence to: Key Laboratory of Mariculture (Ministry of Education), Fisheries College, Ocean University of China, No.5 Yushan Road, Qingdao 266001, China.

E-mail address: lixian@ouc.edu.cn (X. Li).

Highlights

- 120 mg/L PO_4^{3-}-P caused intestine tissue damage, characterized by intercellular spaces.
- The activities of α-amylase, trypsin, and lipase declined with increasing PO_4^{3-}-P concentration.
- 120 mg/L PO_4^{3-}-P caused oxidative stress to intestine.
- 120 mg/L PO_4^{3-}-P exposure reduces intestinal microbiota diversity in turbot.

Abstract

Recirculating aquaculture systems (RAS) have become a key sustainable aquaculture model due to their water-saving and eco-friendly advantages. However, RAS water treatment shows limited phosphate (PO_4^{3-}-P), removal, leading to long-term accumulation that may threaten fish health. The intestine is among the first organs exposed to PO_4^{3-}-P upon seawater ingestion. While PO_4^{3-}-P affects fish growth via mineral metabolism disruption, its specific effects on intestinal health remain unclear. We conducted a 60-day RAS trial exposing juvenile turbot (0, 60, 120 mg/L PO_4^{3-}-P) to assess impacts on intestinal histopathology, digestive function, immunity, and microbiota. Histopathological examination demonstrated that 120 mg/L PO_4^{3-}-P induced severe intestinal lesions, including pronounced intercellular space widening in villi and epithelium, indicating substantial barrier impairment. This structural damage coincided with a paradoxical downregulation of key antioxidant genes (*sod*, *cat*) under high PO_4^{3-}-P conditions, contrasting with their upregulation at 60 mg/L, revealing a critical threshold for oxidative stress defense collapse. Concomitantly, this exposure significantly suppressed digestive enzyme activities (α-amylase, trypsin, lipase; $P < 0.05$), suggesting probable nutrient malabsorption and growth retardation. The microbial community exhibited pathological restructuring, featuring diversity loss and emergence of potentially hazardous populations, including proliferating Cyanobacteria and invasive Deinococcota. In conclusion, chronic exposure to high PO_4^{3-}-P induces intestinal dysfunction in turbot through an oxidative stress-microbial dysbiosis-intestinal structural damage cascade. These interconnected changes demonstrate that

chronic PO_4^{3-}-P accumulation initiates a cascade of intestinal dysfunction, potentially leading to systemic health deterioration, suggesting a warranted PO_4^{3-}-P monitoring in RAS.

Keywords

Digestive enzyme activity; Oxidative stress; Intestinal microbiota;

Introduction

Aquaculture has emerged as an indispensable pillar of global food security, providing humanity with substantial quantities of high-quality aquatic products (FAO 2022). As a vital source of animal protein, modern aquaculture plays an increasingly critical role in the world's food supply system, with its output now constituting an irreplaceable component of human dietary patterns (Tacon et al. 2023). Traditional aquaculture systems face challenges of resource depletion and environmental pollution. Recirculating aquaculture systems (RAS) have emerged as a sustainable alternative due to their water-saving and eco-friendly characteristics (Ahmed & Turchini 2021; Muniz et al. 2015; Zhang et al. 2011). However, water treatment in RAS presents significant technical challenges, particularly regarding the accumulation of nitrogen and phosphorus derived from the dissolution of residual bait and fecal matter. The absorption of environmental phosphate (PO_4^{3-}-P) in the marine teleost intestine is primarily mediated by sodium-dependent phosphate (NaPi) cotransporters (Sugiura. 2024; Sugiura et al. 2004). While this active transport system efficiently maintains phosphorus homeostasis under normal physiological conditions, continuous exposure

63 to abnormally high ambient PO_4^{3-}-P levels in RAS may oversaturate these transport
64 mechanisms, potentially disrupting cellular ionic balance and initiating tissue stress (Li
65 et al. 2025; Wu et al. 2025).

66 However, less is known about the toxicity of PO_4^{3-}-P due to its traditional concept
67 of low toxicity and abundance in natural water. Natural PO_4^{3-}-P levels are typically
68 below 1 mg/L, but in aquaculture systems, such as intensive recirculating systems, the
69 concentrations can reach 25–45 mg/L due to phosphorus-rich feeds and high stocking
70 density (van Bussel et al. 2013). Phosphorus is an important component of aquatic
71 organisms and participates in many biological processes. However, excessive exposure
72 to PO_4^{3-}-P could have tissue damage on aquatic animals. Some research has examined
73 PO_4^{3-}-P toxicity on freshwater fish. The lethal PO_4^{3-}-P dose for juvenile African catfish
74 (*Clarias gariepinus*) was found to be 61 mg/L over 96 hours (Ufodike & Onusiriuka
75 1990). PO_4^{3-}-P toxicity is notable in juvenile common carp (*Cyprinus carpio*) at low
76 concentrations of 0.14 mg/L (Toor et al. 1983). Furthermore, our previous research has
77 demonstrated that juvenile turbot can tolerate PO_4^{3-}-P exposure at concentrations up to
78 60 mg/L. However, under higher stress levels of 120 mg/L, they exhibit irreversible
79 oxidative damage, accompanied by pathological manifestations including gill cell
80 apoptosis and significant histopathological alterations in liver and spleen tissues (Li et
81 al. 2025; Wu et al. 2025).

82 The intestine plays a crucial role in digestion, nutrient absorption, immune
83 function, and overall health maintenance (Knoepfel et al. 2019). Intestinal epithelial
84 cells act as a first line of defense against pathogens, and the intestinal microbiota plays

85 a crucial role in host health by aiding digestion and supporting immune function
86 (Buddington et al. 1997). Disruptions to the intestinal microbiota, can lead to disorders
87 in digestion and absorption, and immune disease risk (Brown 2022). Marine fish
88 generally regulate their osmotic pressure by ingesting seawater, during which the
89 intestine serves as one of the primary organs directly exposed to the seawater.
90 Meanwhile, PO_4^{3-}-P absorption in aquatic animals primarily occurs through the
91 intestinal epithelium. The intestine and gills, as two organs in contact with seawater,
92 have been shown in studies to suffer structural damage to gill tissue and impaired
93 intercellular signaling recognition when exposed to low concentrations of PO_4^{3-}-P (10
94 mg/L). However, short-term acute exposure to PO_4^{3-}-P does not result in significant
95 damage to intestinal tissue (Qi et al. 2023). This prompts the following inquiries: (1)
96 whether the lack of evident histopathological alterations in the intestine under acute
97 exposure can be attributed to the brief duration of exposure; and (2) whether chronic
98 PO_4^{3-}-P exposure can induce toxic effects on the intestine of the turbot, and if so,
99 whether the turbot intestine undergoes adaptive processes in response to PO_4^{3-}-P
100 exposure.

101 When excessive PO_4^{3-}-P enters the circulatory system through gill and intestinal
102 absorption, it may induce systemic oxidative stress through toxicity pathways similar
103 to conventional water pollutants like ammonia and nitrite (Biller & Takahashi 2018;
104 Halliwell 2012; Menon et al. 2023; Soler et al. 2021). During PO_4^{3-}-P-induced oxidative
105 stress, fish intestines initially activate the Nuclear factor erythroid 2-related factor 2
106 signaling pathway (Nrf2 pathway) to upregulate antioxidant enzyme genes, such as

superoxide dismutase (*sod*), *catalase* (*cat*), and *glutathione peroxidase* (*gpx*) in response to ROS overaccumulation - where Sod converts superoxide anions (O^{2-}) to H_2O_2, while Cat and Gpx further break down H_2O_2 into water to maintain redox homeostasis (Yan et al. 2021). However, when PO_4^{3-}-P concentrations exceed safe thresholds, sustained oxidative pressure suppresses the Nrf2 pathway, accompanied by downregulation of *sod*/*cat*/*gpx* expression and reduced enzymatic activity. This impairs ROS clearance and exacerbates oxidative damage, subsequently triggering apoptosis pathways while significantly inhibiting both activity and gene expression of digestive enzymes (α-amylase, trypsin, and lipase). This compromised state, coupled with a concurrent disruption of the intestinal microbiota—namely a reduction in beneficial microbes and an increase in harmful ones, ultimately causing intestinal digestive dysfunction. This oxidative stress-mediated cascade culminates in structural intestinal damage, impaired nutrient absorption, and growth performance reduction. Therefore, comprehensive assessment of oxidative stress responses, tissue damage and function is critical for evaluating PO_4^{3-}-P toxicity and characterizing fish adaptive recovery mechanisms.

Turbot is considered a worldwide fish species of significant economic value. The growth, reproduction, and overall health are highly susceptible to environmental pollution, primarily due to its limited swimming ability and restricted range of activity. Our previous investigation has demonstrated that a concentration of 60 mg/L of PO_4^{3-}-P induces acute toxic effects in turbot, manifesting as intestinal tissue damage and stress responses. Notably, this concentration did not result in mortality among juvenile turbot.

Consequently, the current study seeks to examine: 1) the potential for turbot to adapt to prolonged exposure to this PO_4^{3-}-P concentration under aquaculture conditions; 2) Whether higher concentrations of PO_4^{3-}-P would induce toxic effects on turbot following prolonged exposure. This study conducted a 60-day experiment using PO_4^{3-}-P solutions at concentrations of 0, 60, and 120 mg/L to investigate their effects on turbot intestinal histology, immunity, digestive enzyme activity, and intestinal microbiota. The findings provide new insights into the mechanisms of PO_4^{3-}-P toxicity in marine teleost fish and offer valuable recommendations for water quality management in aquaculture.

Materials and methods

Experimental animals

Juvenile turbot (initial body weight: 41.23 ± 2.97 g; initial body length: 11.47 ± 0.23 cm) were provided by Shenghang Aquatic Technology Co., Ltd. (Weihai, China). A total of 450 healthy, uninjured, and highly active individuals were obtained and acclimated to the laboratory conditions for two weeks prior to the experiment. Throughout the experiment, juvenile turbot were fed a commercial pellet diet (Qingdao Longxing Feed Co., Ltd., Shandong, China), consisting of 50% crude protein, 10% crude lipids, 16.5% crude ash, 5.0% crude fiber, 12% moisture, 1.5% calcium, 0.5% phosphorus, and 2.2% amino acids. The initial feeding rate was set at 8% of their body weight, with adjustments made based on weight changes. Feeding occurred twice daily

149 at 08:00 and 16:00. The health and condition of the juvenile turbot were closely
150 monitored on a daily basis to ensure their well-being. All animal experimental protocols
151 were reviewed and approved by the Animal Ethics Committee of Ocean University of
152 China (Approval No. OUC-AE-2025-309).

153 **Experimental design**

154 The research was carried out using nine small recirculating water systems, each
155 equipped with a rearing tank, a two-stage biofilter tank, a UV sterilizer, an oxygen
156 diffuser, and a low-suction circulation pump. The systems were divided into three
157 concentration groups: 0 mg/L (control group, CK), 60 mg/L (low concentration group,
158 LP), and 120 mg/L (high concentration group, HP). Each group comprised three
159 replicate experimental systems. Following the two-week acclimation period, the 450
160 juvenile turbot were randomly and equally distributed into the nine rearing tanks,
161 resulting in 50 fish per tank. At the time of sampling, three fish were randomly collected
162 from each rearing tank. The treatment groups' PO_4^{3-}-P concentrations were achieved by
163 blending disodium hydrogen phosphate (Na_2HPO_4) and monosodium dihydrogen
164 phosphate (NaH_2PO_4) in a 3:1 ratio. According to relevant literature, the sodium-to-
165 potassium ion ratio in natural seawater is 21:1 (Romano & Zeng, 2009). Sodium ions
166 and potassium chloride (KCl) were added to ensure that sodium-to-potassium ion ratio
167 was similar to that of natural seawater at 21:1.

Water quality analysis

Throughout the experiment, water quality was rigorously monitored. A handheld multiparameter water quality analyzer (manufactured by YSI, USA) was used to measure dissolved oxygen (DO), temperature (T), salinity (S), and pH every 12 hours. Additionally, total ammonia nitrogen (TAN), nitrate nitrogen (NO_3^--N), nitrite nitrogen (NO_2^--N), and PO_4^{3-}-P were measured every 24 hours using Nessler's reagent colorimetry, phenol disulfonic acid spectrophotometry, sulfanilamide method, and phosphomolybdenum blue colorimetry, respectively (Yu et al. 2021). The above mentioned parameters exhibited no significant differences.

Sample collection

The experiment spanned 60 days, with feeding discontinued on the 58th day to ensure complete intestinal clearance in the juvenile turbot. At the time of sampling, three juveniles were randomly selected from each rearing tank. Totally, nine juvenile turbot were randomly sampled from each treatment group. Anesthesia was induced with a 0.05% solution of tricaine methane sulfonate (MS-222, Sigma Diagnostics INS, St. Louis, MO), and their body length and weight were recorded. The fish were then expeditiously dissected to harvest and weigh the intestinal tissue, which was subsequently cleansed with sterile saline and fixed in Bouin's solution for a duration of 24 hours. After fixation, replace the solution with 70% ethanol and store at 4 ℃ for subsequent histopathological examination. Additionally, samples cryopreserved in liquid nitrogen will be used for

subsequent analyses, including digestive enzyme and oxidative stress enzyme activity assays, gene expression profiling, and intestinal microbial community sequencing.

Histopathology observation

Intestinal tissues were immersed in Bouin's fixative for a 24-hour period, subsequent to which they underwent dehydration in a graded series of ethanol solutions. Following equilibration in xylene, the specimens were embedded in paraffin for the preparation of 5 μm tissue sections. Hematoxylin and eosin (HE) staining was employed to colorize the intestinal slides, which were then examined microscopically (Slaoui & Fiette 2011). The morphological characteristics of the intestines were quantified utilizing the NIS-Elements image analysis software (Nikon, Japan), with photographs taken for documentation purposes.

Determination and analysis of digestive enzyme activities

Enzymatic activities were assessed in tissue samples from each treatment group. The samples were homogenized using a 0.9% NaCl solution at a 1;9 dilution ratio. Subsequently, the homogenates were subjected to centrifugation at 4 ℃ at 2500 g for a duration of 10 min. Following centrifugation, the resulting supernatants were stored at -80 °C in preparation for subsequent utilization. The activities of α-amylase, lipase, and trypsin were subsequently measured using colorimetric methods with α-amylase assay kit (catalog number C 016-1-1), lipase assay kit (catalog number A054-1-1), and trypsin assay kit (catalog number A080-2-2) provided by Nanjing Jiancheng Bioengineering

Institute, respectively, following with the manufacturer's protocols.

Quantitative Real-time PCR

Total RNA was extracted from turbot intestinal tissues using the RNA extraction kit (RC113-01, Vazyme, Nanjing, China), followed by cDNA synthesis using the HiScript® III RT SuperMix for qPCR (+gDNA wiper) kit (Vazyme, Nanjing, China) according to the manufacturer's protocol. NCBI-designed primers targeting oxidative stress-related genes (listed in Table 1, obtained from GenBank and synthesized by Qingdao Tsingke Biotechnology Co.), with *18s* rRNA as the internal reference gene, were first validated through standard curve and melt curve analyses to confirm primer specificity and amplification efficiency prior to RT-qPCR. Quantitative PCR was then performed using the Takara TB Green™ Premix Ex Taq™ II (Tli RNaseH Plus) (RR 820A) kit on a real-time PCR system with a 20 μL reaction volume under the following conditions: initial denaturation at 95 ℃ for 30 sec, followed by 40 cycles of 95 ℃ for 5 sec and 60 ℃ for 30 sec. Relative mRNA expression levels were ultimately calculated using the $2^{-\Delta\Delta Ct}$ method (Livak & Schmittgen 2001).

Bacterial DNA extraction, amplification, sequencing, and bioinformatics analysis

Juvenile turbot were dissected in aseptic conditions, and the entire intestine were collected into sterile containers to fulfill the needs of subsequent experiments. Subsequently, total genomic DNA was meticulously extracted from the intestinal samples in accordance with the manufacturer's protocols. The extracted DNA samples were subsequently dispatched to Majorbio Bio-Pharm Technology Co. Ltd., situated in Shanghai, China, where PCR amplification was performed and the subsequent generation of Illumina sequencing libraries was undertaken. The V3-V4 hypervariable region of the *16s* rRNA gene was targeted for amplification using the specific primer set F338/R806. Following stringent quality control, the amplified libraries were sequenced on the Illumina platform to generate 300bp paired-end reads. Post-sequencing, raw read data was subjected to quality filtering and assembly using FASTP (version 0.19.6) and FLASH software (version 1.2.11). Processed sequences with a minimum of 97% similarity were then clustered into operational taxonomic units (OTUs) with UPARSE software (version 11). The classification of each OTU was further delineated using the RDP Classifier (version 2.13) in conjunction with the SILVA database (version 138).

Statistical analysis

Statistical analysis of the data was conducted using SPSS 22.0 software. All data are presented as mean ± standard deviation (SD), and one-way ANOVA was performed

along with Duncan's multiple comparison test, with the significance level at $P < 0.05$.

Results

Intestine tissue histopathology

Upon examination of the intestinal tissues across varying PO_4^{3-}-P concentrations, as depicted in Fig. 1A-C, no histological abnormalities were detected in the CK and LP. The intestinal epithelial cells were densely arranged, exhibiting consistent size and, with the villi's lamina propria maintaining a robust attachment to the epithelium. Contrarily, in the HP, certain epithelial cells displayed minute cavities, and the villi exhibited serrated edges indicative of damage, accompanied by the presence of significant cavities within. To further quantify these morphological alterations, intestinal villus width and muscularis thickness were measured (Fig. 1D, 1E). Consistent with the qualitative histological observations, the HP exhibited a significant reduction in both villus width and muscularis thickness compared to the CK and LP ($P < 0.05$). In contrast, no significant morphological differences were observed between the LP and CK, indicating that intestinal structural integrity was preserved at 60 mg/L PO_4^{3-}-P.

Intestinal oxidative stress status

The varying PO_4^{3-}-P concentrations influenced the Sod activity within the intestines of juveniles. Following a 60-day exposure to PO_4^{3-}-P, the Sod activity in the intestines of

the LP group exhibited no significant departure from that of the CK group, whereas a significant reduction in Sod activity was observed in the HP group. Correspondingly, prolonged exposure to high PO_4^{3-}-P concentrations resulted in a significant decrease in the activities of both Cat and Gpx in the intestines of the juvenile fish when compared to the CK group (Fig. 2).

Gene expression associated with oxidative stress, including *mn-sod*, *cu/zn-sod*, *cat*, and *nrf2*, varied across the PO_4^{3-}-P treatment groups (Fig. 3). The *mn-sod* expression level was reduced in the HP, yet no significant divergence from the CK and LP was noted. Conversely, *cu/zn-sod* expression significantly elevated in the HP when contrasted with the CK. Moreover, the mRNA expression of the *cat* gene was significantly upregulated with LP compared to the CK, while high concentrations yielded a decrease. The LP demonstrated a significantly augmented *nrf2* expression compared to both the CK and HP. Although the *nrf2* level was reduced in the HP versus the CK, this decrement was not statistically significant.

Digestive enzyme activities

α-Amylase activity was notably diminished in the HP treatment group compared to the CK. Conversely, no statistically significant disparities in α-amylase activity were detected between the LP treatment group and the CK. Similar patterns were observed for the activities of trypsin and lipase, which exhibited significant reductions in the HP but were unaffected in the LP (Fig. 4).

Intestinal microbiota

Under varying PO_4^{3-}-P concentration stressors, α and β diversities of the intestinal microbial communities were quantified at the operational taxonomic unit (OTU) level (Table 2 and Fig. 5B). The microbial communities in the CK and low LP groups exhibited greater richness than those in the high HP group. The LP group demonstrated reduced diversity compared to both the CK and HP groups. A Venn diagram revealed 23 shared OTUs among the CK, LP, and HP groups. Unique OTUs numbered 75 for CK, 95 for LP, and 65 for HP (Fig. 5A). The mean number of OTUs in the HP group was inferior to that observed in the other two groups, aligning with the lower Chao and Ace indices in the α-diversity index table (Table 2). Principal coordinate analysis (PCoA) plot (Fig. 5B), with principal components 1 and 2 accounting for 75.41% and 15.89% of the variance respectively, revealed distinct patterns of community dispersion. Notably, while the samples in the CK and LP groups clustered relatively tightly with small intra-group variation, the HP group exhibited substantial intra-group dispersion. This pronounced individual variation within the HP group indicates that extreme PO_4^{3-}-P stress (120 mg/L) severely destabilized the intestinal microbial community, leading to significant structural dysbiosis and individualized chaos rather than a uniform community shift.

An analysis at the phylum level revealed that the dominant microbial taxa across different PO_4^{3-}-P concentration treatment groups exhibited similarities, with the majority comprising Proteobacteria, Cyanobacteria, Firmicutes, Actinobacteria, and Deinococcus-Thermus. These phyla accounted for 85%–95%, 3%–11%, 1%–2%, 1%–

2%, and 0%–1% of the total sequences, respectively (Fig. 6A). The turbot intestine harbored two predominant phyla: Proteobacteria and Cyanobacteria (Fig. 6C). Within the three treatment groups (CK, LP, and HP), the Proteobacteria in the HP group demonstrated a lower relative abundance compared to the CK and LP groups. Conversely, the relative abundance of Cyanobacteria was notably enhanced under conditions of high PO_4^{3-}-P stress (Fig. 6C). Furthermore, Deinococcus-Thermus was absent in the CK group, a contrast to its presence in both the LP and HP groups.

Analysis at the genus level identified *Achromobacter*, *Sphingomonas*, *Deinococcus*, *Kocuria*, and *Staphylococcus* as the top five dominant genera within the turbot's intestinal microbial community. Moreover, chlorophyll concentrations were elevated across all three treatment groups, as depicted in Fig. 6D. The genus-level assessment of the intestinal microbial community indicated variances among the treatment cohorts (Fig. 6B and 6D). The HP group exhibited a reduced relative abundance of *Achromobacter* when compared to the CK and LP groups. A tendency toward greater chlorophyll abundance was observed under high PO_4^{3-}-P stress conditions. Additionally, the control group presented a higher relative abundance of *Kocuria* compared to both the low and high PO_4^{3-}-P treatment groups.

Discussion

Elevated PO_4^{3-}-P levels in aquaculture environments, which was often caused by overfeeding in high-density fish farming and the water pollution caused by the discharge of urban and industrial wastewater, can significantly impact fish health (Zong

et al. 2017). As a major component of wastewater, excessive PO_4^{3-}-P has the potential to disrupt intestinal metabolism and alter the intestinal microbiota of fish. Given the crucial role of intestinal microbiota in immune function and its intricate diversity, our current understanding of how PO_4^{3-}-P exposure affects fish intestinal microbiota remains incomplete. Therefore, studying the intestinal microbiome of fish under high-PO_4^{3-}-P conditions is essential for enhancing their immune resilience and developing effective strategies for disease prevention and treatment in aquaculture systems.

This study examined the potential toxic impacts of PO_4^{3-}-P on fish intestine by exposing juvenile turbot to varying concentrations of PO_4^{3-}-P. The objective was to elucidate the mechanisms by which PO_4^{3-}-P can affect fish intestinal health. Long-term exposure to a PO_4^{3-}-P concentration of 60 mg/L did not cause significant damage to the intestinal tissue of turbot. In contrast, exposure to a higher PO_4^{3-}-P concentration (120 mg/L) led to pathological changes in the intestinal tissue, characterized by epithelial cell damage and vacuolation, serrated lesions in the intestinal villi, and the formation of numerous cavities. Furthermore, the quantitative morphometric analysis revealed a significant reduction in both intestinal villus width and muscularis thickness under 120 mg/L PO_4^{3-}-P exposure. The intestinal villi are critical functional structures for nutrient assimilation; thus, a decrease in their width directly contracts the absorptive surface area, which strongly correlates with the observed decline in digestive enzyme activities. Concurrently, the significant thinning of the muscularis layer indicates a severe weakening of the intestinal structural integrity and peristaltic capacity. These combined morphological impairments suggest that extreme PO_4^{3-}-P accumulation not only

damages the epithelial barrier but also mechanically compromises the gastrointestinal motility, ultimately driving nutrient malabsorption.

Previous studies have demonstrated that higher concentrations of pollutants can induce intestinal tissue injury. For instance, simultaneous exposure to cadmium and nitrates has the potential to induce intestinal damage in flounder, while exposure to either cadmium or nitrates alone can similarly result in such damage in aquatic organisms (P. F. Liu et al. 2023). Previous studies have robustly demonstrated a significant relationship between the histological alterations observed in intestinal tissue and the presence of pollutants which are closely associated with oxidative stress (Lushchak 2016). Under common physiological conditions, the cellular production and scavenging of reactive oxygen species ROS are meticulously balanced, with optimal ROS levels playing a crucial role in modulating cellular functions and gene expression (Jomova et al. 2024). However, when exposed to pollutant-induced stress, fish experience an oxidative stress response, characterized by an overflow of ROS (Gao et al. 2024). This surge in ROS overwhelms the antioxidative defense mechanisms, triggering a cascade of cellular and tissue-level physiological and pathological reactions that can lead to severe outcomes, including the impairment of cellular function, apoptosis, and necrosis (Dröge 2002; Thannickal & Fanburg 2000).

Therefore, it was further investigated the oxidative stress response status of turbot juveniles under the exposure to various PO_4^{3-}-P concentration. Environmental pollutants are important factors contributing to oxidative stress responses. It has been demonstrated that microplastics can interfere with the endocrine system of fish,

eliciting oxidative stress reactions (Qiao et al. 2019). Similarly, nitrite poisoning has been shown to induce oxidative stress while stimulating the activation of the antioxidant defense mechanism. To mitigate this impact, the physiological response in fish involves the activation of the antioxidant enzyme system, which includes genes such as *nrf2*, *sod*, and *cat*, along with enzymes like Sod, Cat, and Gpx. In this study, significant variations in the mRNA levels of antioxidant genes associated with elevated PO_4^{3-}-P concentrations were observed. The *nrf2* (Nuclear factor erythroid 2-related factor 2) gene, functioning as a transcription factor, is integral to the cellular response to oxidative stress and electrodysfunction (Kensler et al. 2007). Under oxidative stress, *nrf2* activates the expression of downstream antioxidant genes associated with the antioxidant response element (ARE), including *sod*, *cat*, and others (Uruno & Motohashi 2011). Under the current experimental conditions, exposure to 60 mg/L PO_4^{3-}-P may induce physiological stress in juvenile flounder, resulting in upregulation of *nrf2* gene expression. As the master regulator of oxidative stress responses, *nrf2* plays a central role in enhancing *cat* gene expression when activated. This upregulation leads to increased production of *cat*, which effectively breaks down hydrogen peroxide and significantly reduces intracellular ROS accumulation, thereby protecting juvenile flounder from oxidative damage. However, sustained exposure to elevated PO_4^{3-}-P concentrations may ultimately overwhelm this protective mechanism, potentially leading to oxidative damage through disruption of antioxidant enzyme homeostasis and subsequent downregulation of both *nrf2* and *cat* gene expression. As the primary isoforms of the *sod* gene, *cu/zn-sod* and *mn-sod* play a critical role in combating

391 oxidative stress in organisms (Carlioz & Touati 1986; Lefaix et al. 1996). Specifically,
392 *sod*, comprising both cytoplasmic and extracellular variants, is a pivotal scavenger of
393 free radicals in response to oxidative stress (Abreu & Cabelli 2010; Li et al. 2010).
394 During instances of oxidative stress, *nrf2* gene can catalyze the synthesis of superoxide
395 dismutase by activating the *sod* gene. This upregulation of *sod* gene expression within
396 cells is instrumental in mitigating ROS-induced damage to the organism (Cheng et al.
397 2006; Oberley & Buettner 1979). At a PO_4^{3-}-P concentration of 60 mg/L, the SOD
398 system is mobilized, counteracting the surplus ROS generated by oxidative stress
399 through augmented expression of *cu/zn-sod* and *mn-sod* genes. This response is
400 characterized by a notable upsurge in gene expression within the intestines of juvenile
401 fish. Conversely, in the 120 mg/L stress group, the intestines of juvenile turbot exhibited
402 a decline in *mn-sod* gene expression, concurrent with a substantial escalation in the
403 expression of the *cu/zn-sod* gene. Following 60 days of chronic exposure, the
404 suppression of *mn-sod* likely represents a decompensation stage of the antioxidant
405 defense system. The sustained oxidative injury inflicted by elevated PO_4^{3-}-P
406 concentrations appears to have overwhelmed the mitochondrial antioxidant capacity,
407 leading to increased mitochondrial production of superoxide radicals. Consequently,
408 the heightened expression of *cu/zn-sod* acts as a secondary defense to counteract this
409 severe superoxide leakage. This shift triggers the RAS-dependent ROS signaling
410 pathway, orchestrating a negative feedback regulation that influences the opposing
411 changes in sod gene expression in an attempt to manage the extensive damage arising
412 from disrupted metabolic processes. Previous studies have demonstrated that the

intestine of pufferfish exposed to 5 mg/L cadmium exhibits a higher relative expression of the *cu/zn-sod* gene compared to the *mn-sod* gene, aligning with the observations of the present study (Kim et al. 2010). Additionally, our findings demonstrate distinct adaptive responses between exposure groups. The LP group exhibited successful acclimation through upregulation of relevant gene expression, whereas the HP group showed compromised antioxidant defense capacity due to PO_4^{3-}-P-induced oxidative stress. Specifically, the high-concentration PO_4^{3-}-P exposure disrupted redox homeostasis, leading to significant downregulation of key antioxidant genes.

In the current study, the enzymatic activities of Sod, Cat, and Gpx remained unchanged in the 60 mg/L treatment group, whereas a significant decline was noted in the 120 mg/L treatment group. This may be attributed to the fact that PO_4^{3-}-P stress at 60 mg/L triggered the antioxidant defense mechanisms in juvenile fish. Compared to the CK, juvenile turbot in the LP group maintained relatively stable levels of Cat and Sod enzymes, suggesting successful acclimation to this PO_4^{3-}-P concentration. In contrast, HP group specimens exposed to elevated PO_4^{3-}-P concentrations exhibited compromised antioxidant defense systems, as evidenced by significant downregulation of critical antioxidant enzymes including Cat. This dysregulation impaired the maintenance of enzymatic equilibrium among Cat, Sod, and related antioxidant enzymes, ultimately leading to immunosuppression and disruption of normal physiological functions in the exposed juveniles. This study propose that higher PO_4^{3-}-P concentrations can impose stress on organisms, potentially triggering oxidative stress responses and activating corresponding antioxidant defense mechanisms (Coskun et al.

435 2001). Furthermore, these enzymes have the capability to remove superoxide anion
436 radicals and hydrogen peroxide, consequently restoring and preserving the body's
437 oxidative stress equilibrium and mitigating ROS-induced damage to cells and tissues
438 (Liu et al. 2022). Histological analysis confirmed preserved intestinal integrity in the
439 LP group without pathological alterations. In contrast, the HP group showed markedly
440 reduced expression of oxidative stress-related genes accompanied by significant
441 intestinal tissue damage. Prolonged contaminant exposure may induce ROS-mediated
442 oxidative sequelae, causing irreversible protein damage that compromises antioxidant
443 defenses, cellular function, and viability. To counteract this damage, organisms have
444 evolved cellular stress responses to maintain physiological homeostasis (Padmini 2010).
445 However, excessive stress ultimately overwhelms regulatory and immune-protective
446 mechanisms, leading to physiological dysregulation and potentially lethal outcomes in
447 fish (Selye 1950).

448 Digestive enzyme activity is a critical metric for ascertaining an organism's
449 capacity for nutrient absorption and growth promotion (Liu et al. 2024). The present
450 study revealed that PO_4^{3-}-P exposure at a concentration of 60 mg/L did not produce
451 notable alterations in the activity of key digestive enzymes (α-amylase, lipase, and
452 trypsin) relative to the control group. However, a significant reduction in the activity of
453 these enzymes was observed in turbot treated with 120 mg/L PO_4^{3-}-P. The activity of
454 digestive enzymes is closely linked to the health of intestinal cells and tissues. Studies
455 have found that oxidative stress and inflammatory responses induced by high
456 concentrations of pollutants can damage cells and tissues, potentially leading to a

457 decline in the synthesis and secretion of digestive enzyme. Moreover, the ROS
458 generated by oxidative stress can alter the surface properties and active sites of enzyme
459 proteins, potentially leading to the reduction in their activity (Wang et al. 2012). Turbot
460 juveniles in the LP group adapted well to 60 mg/L PO_4^{3-}-P exposure, maintaining tissue
461 integrity without excessive ROS accumulation, which preserved normal digestive
462 enzyme production and activity. However, at HP group, the antioxidant system was
463 overwhelmed, leading to oxidative stress-induced tissue damage, ROS buildup, and
464 consequently, impaired digestive enzyme function. The significant suppression of α-
465 amylase, trypsin, and lipase activities under 120 mg/L PO_4^{3-}-P exposure suggests a
466 severe impairment of nutrient digestion capacity. This biochemical dysfunction is
467 highly consistent with the significant growth retardation observed in the same cohort
468 of fish reported by Li et al. (2025). The reduction in digestive efficiency likely serves
469 as a primary driver for the diminished growth performance under high-PO_4^{3-}-P stress.
470 The intestine is the habitat to a variegated microbial community that is critical in
471 upholding intestinal immune functionality and the well-being of the host organism (Yu
472 et al. 2024; Zengler & Zaramela 2018). Extensive research has indicated that
473 environmental pollutants can disturb the ecological equilibrium of the intestinal
474 microbiota (Mustafa et al. 2024). This study revealed marked variations in the
475 abundance and diversity of the intestinal microbial community across different PO_4^{3-}-P
476 concentrations. Notably, exposure to 120 mg/L of PO_4^{3-}-P resulted in a decreased
477 richness of the microbial community, while the 60 mg/L PO_4^{3-}-P exposure group also
478 exhibited significant changes in community diversity. The integrity of microbial

abundance and diversity is crucial for sustaining the homeostasis of the host's internal milieu, and any decrement in these parameters may perturb the intestinal microbial balance, thereby enhancing the risk of pathogen infection in the host (Bernardini et al. 2021; Chang et al. 2023; Cooper et al. 2021). Consequently, the decrease in microbial community richness induced by PO_4^{3-}-P exposure may imperil the health of juvenile turbot.

Microbial phylum-level analysis revealed significant shifts in the HP group, most notably the lowest relative abundance of Proteobacteria - a phylum crucial for intestinal food breakdown, nutrient synthesis, and pathogen defense in fish (Cardona et al. 2016; Morrison et al. 2009). This reduction may disrupt intestinal microbiota equilibrium, impairing digestive efficiency and nutrient absorption while potentially compromising immune defenses against pathogens (Shui et al. 2020). Conversely, Cyanobacteria dominated the HP group, likely due to their phosphorus-utilizing capacity (Lewin et al. 2003) and introduction through natural seawater ingestion during respiration and feeding (Zimmer et al. 2006; Ghanbari et al. 2015). While ecologically important in aquatic systems (Head et al. 1999), certain Cyanobacteria produce harmful toxins (microcystins, cyclic lipopeptides) that induce oxidative stress, cellular damage, and health complications (Mereish & Solow 1990; Rymuszka et al. 2007; Zhang et al. 2006). The increased cyanobacteria abundance in the HP group suggests high PO_4^{3-}-P concentrations disrupted intestinal microbial equilibrium, which further manifested as oxidative stress dysregulation (with significantly decreased Cat and Sod activity) and intestinal tissue damage. correlating with observed oxidative dysregulation (reduced

CAT/SOD activity) and intestinal tissue damage in PO_4^{3-}-P-stressed fish. The CK group maintained higher Firmicutes abundance, which supports fish health through production of beneficial short-chain fatty acids (SCFAs) that regulate energy metabolism and provide anti-inflammatory/antioxidative benefits (Bertolini et al. 2022; Cai et al. 2022). The HP group's Firmicutes depletion suggests 120 mg/L PO_4^{3-}-P exposure disrupted microbial balance, while the rare detection of radiation-resistant Deinococcota - atypical in intestinal environments (Blasius et al. 2008) - may reflect pH elevation from PO_4^{3-}-P stress, as its abundance appears pH-dependent (Wang et al. 2023), though its intestinal role remains poorly understood.

At the genus level, the abundance of *Achromobacter* was lower in the HP group compared to the control. *Achromobacter* species are considered to have a low pathogenic potential, and their specific role in fish intestines remains unclear. However, they may interact with other pathogenic microbes, potentially exacerbating the detrimental effects of pathogens like certain *Staphylococcus* species on fish intestinal tissues (Azevedo et al. 2016). Moreover, the higher chlorophyll content observed in the HP group relative to the CK and LP groups supports the notion that increased Cyanobacteria abundance may negatively impact the intestines of juvenile turbot.

The current study proved that 120 mg/L PO_4^{3-}-P exposure caused the impaired function of intestine of turbot, characterized by tissue damage, oxidative stress, inhibited digestive enzymes activities and intestinal microbiota disorders. The disfunction of intestine could further compromise nutrient absorption efficiency, ultimately resulting in growth retardation. LP showed no significant effect on growth

performance. In contrast, turbot juveniles showed adaptation to the 60 mg/L PO_4^{3-}-P, with no obvious disfunction of intestine and growth retardation observed (Li et al. 2025). Therefore, in RAS of high stocking density conditions, it is necessary to closely monitor PO_4^{3-}-P accumulation. Turbot can be safely cultivated at a PO_4^{3-}-P concentration of 60 mg/L.

Conclusion

In conclusion, the data analysis from the current study indicates that juvenile turbot demonstrated adaptation to exposure of 60 mg/L PO_4^{3-}-P, with no significant adverse effects observed on their physiological well-being. Conversely, 120 PO_4^{3-}-P levels induce damage to the intestinal epithelial villi and cells, markedly diminishing digestive enzyme activity in the intestine and significantly reducing the expression of genes associated with antioxidant defense. Moreover, the study's findings indicate that prolonged exposure to 120 mg/L PO_4^{3-}-P concentrations can disturb the intestinal microbial community in turbot, potentially escalating the vulnerability of marine teleost fish to pathogenic infiltration. Prolonged exposure to elevated levels of PO_4^{3-}-P, attributable to phosphate accumulation in RAS, has the potential to adversely affect the intestinal health of turbot.

Author Contribution Jiale Zhou and Lele Wu contributed equally to this work. Jiale Zhou: Conceptualization, Visualization, Validation, Data curation, Formal analysis, Writing - original draft. Lele Wu: Conceptualization, Visualization, Software, Writing - review & editing. Xin Li: Supervision. Xiangyu Zhang: Investigation, Methodology, Data curation. Ting Qi: Methodology, Resources. Xian Li: Conceptualization, Visualization, Supervision, Project administration, Funding acquisition, Writing - review & editing.

Funding This study was supported by the National Natural Science Foundation of China (32273104, 42461160255).

Data Availability The raw data supporting the findings of this study are available from the corresponding author (X. Li, lixian@ouc.edu.cn) upon reasonable request.

Declarations

Competing Interest The authors declare that they have no known competing financial interests or personal relationships that could have appeared to influence the work reported in this paper.

References

Abreu IA, Cabelli DE (2010) Superoxide dismutases-a review of the metal-associated mechanistic variations. Biochim. Biophys. Acta 1804(2):263–274. https://doi.org/10.1016/j.bbapap.2009.11.005.

Ahmed N, Turchini GM (2021) Recirculating aquaculture systems (RAS): Environmental solution and climate change adaptation. J. Clean. Prod. 297:126604. https://doi.org/10.1016/j.jclepro.2021.126604.

Azevedo AS, Almeida C, Pereira B, Melo LF, Azevedo NF (2016) Impact of Delftia tsuruhatensis and Achromobacter xylosoxidans on Escherichia coli dual-species biofilms treated with antibiotic agents. Biofouling 32(3): 227–241. https://doi.org/10.1080/08927014.2015.1124096.

Bernardini I, Matozzo V, Valsecchi S, Peruzza L, Dalla Rovere G, Polesello S et al (2021) The new PFAS C6O4 and its effects on marine invertebrates: First evidence of transcriptional and microbiota changes in the Manila clam

Ruditapes philippinarum. Environ. Int. 152:106484. https://doi.org/10.1016/j.envint.2021.106484.
Bertolini A, Fiorotto R, Strazzabosco M (2022) Bile acids and their receptors: modulators and therapeutic targets in liver inflammation. Semin. Immunopathol. 44(4):547–564. https://doi.org/10.1007/s00281-022-00935-7.
Biller JD, Takahashi LS (2018) Oxidative stress and fish immune system: phagocytosis and leukocyte respiratory burst activity. An. Acad. Bras. Cienc. 90(4):3403–3414. https://doi.org/10.1590/0001-3765201820170730.
Blasius M, Sommer S, Hübscher U (2008) Deinococcus radiodurans: what belongs to the survival kit? Crit. Rev. Biochem. Mol. Biol. 43(3):221–238. https://doi.org/10.1080/10409230802122274.
Brown RB (2022）Obesity and cancer: Potential mediation by dysregulated dietary phosphate. Obesities 2(1):64–75. https://doi.org/10.3390/obesities2010007.
Buddington RK, Krogdahl A, BakkeMcKellep AM (1997) The intestines of carnivorous fish: structure and functions and the relations with diet. Acta Physiol. Scand. 161:67–80. https://doi.org/10.1111/j.1469-7793.1997.489be.x.
Cai J, Sun LL, Gonzalez FJ (2022) Gut microbiota-derived bile acids in intestinal immunity, inflammation, and tumorigenesis. Cell Host Microbe 30(3):289–300. https://doi.org/10.1016/j.chom.2022.02.004.
Cardona E, Gueguen Y, Magré K, Lorgeoux B, Piquemal D, Pierrat F et al (2016) Bacterial community characterization of water and intestine of the shrimp Litopenaeus stylirostris in a biofloc system. BMC Microbiol. 16(1):157. https://doi.org/10.1186/s12866-016-0770-z.
Carlioz A, Touati D (1986) Isolation of superoxide dismutase mutants in Escherichia coli: is superoxide dismutase necessary for aerobic life? EMBO J. 5(3):623–630. https://doi.org/10.1002/j.1460-2075.1986.tb04256.x.
Chang XL, Kang MR, Feng JC, Zhang JX, Wang XF (2023) Effects of BDE-209 exposure on growth performance, intestinal digestive enzymes, and intestinal microbiome in common carp (*Cyprinus carpio L.*). Aquac. Fish. 8(1): 33–41. https://doi.org/10.1016/j.aaf.2021.05.005.
Cheng WT, Tung YH, Liu CH, Chen JC (2006) Molecular cloning and characterisation of cytosolic manganese superoxide dismutase (cytMn-SOD) from the giant freshwater prawn Macrobrachium rosenbergii. Fish Shellfish Immunol. 20(4):438–449. https://doi.org/10.1016/j.fsi.2005.05.016.
Cooper RO, Vavra JM, Cressler CE (2021) Targeted manipulation of abundant and rare taxa in the *Daphnia magna* microbiota with antibiotics impacts host fitness differentially. mSystems 6(2):e00916-20. https://doi.org/10.1128/mSystems.00916-20.
Coskun A, Uzunkoy A, Duzgun SA, Bozer M, Ozardali I, Vural H (2001) Experimental sodium phosphate and polyethylene glycol induce colonic tissue damage and oxidative stress. Br. J. Surg. 88(1):85–89. https://doi.org/10.1046/j.1365-2168.2001.01608.x.
Dröge W (2002) Free radicals in the physiological control of cell function. Physiol. Rev. 82(1):47–95. https://doi.org/10.1152/physrev.00018.2001.

611 FAO (2022) The state of world fisheries and aquaculture 2022.
612 https://doi.org/10.4060/cc0461en.
613 Gao F, Zhao YJ, Shi XW, Qiao D, Pei C, Kong XH (2024) Signalling regulation of
614 reactive oxygen species in fish inflammation. Rev. Aquac. 16(3):1266–1285.
615 https://doi.org/10.1111/raq.12895
616 Ghanbari M, Kneifel W, Domig KJ (2015) A new view of the fish gut microbiome:
617 Advances from next-generation sequencing. Aquaculture 448:464–475.
618 https://doi.org/10.1016/j.aquaculture.2015.06.033.
619 Halliwell B (2012) Free radicals and antioxidants: updating a personal view. Nutr. Rev.
620 70(5):257–265. https://doi.org/10.1111/j.1753-4887.2012.00476.x.
621 Jomova K, Alomar SY, Alwasel SH, Nepovimova E, Kuca K, Valko M (2024) Several
622 lines of antioxidant defense against oxidative stress: antioxidant enzymes,
623 nanomaterials with multiple enzyme-mimicking activities, and low-molecular-
624 weight antioxidants. Arch. Toxicol. 98(5):1323–1367.
625 https://doi.org/10.1007/s00204-024-03696-4.
626 Kensler TW, Wakabayashi N, Biswal S (2007) Cell survival responses to environmental
627 stresses via the Keap1-Nrf2-ARE pathway. Annu. Rev. Pharmacol. Toxicol.
628 47:89–116. https://doi.org/10.1146/annurev.pharmtox.46.120604.141046.
629 Kim JH, Rhee JS, Lee JS, Dahms HU, Lee J, Han KN, Lee JS (2010) Effect of cadmium
630 exposure on expression of antioxidant gene transcripts in the river pufferfish,
631 *Takifugu obscurus* (Tetraodontiformes). Comp. Biochem. Physiol. C Toxicol.
632 Pharmacol. 152(4):473–479. https://doi.org/10.1016/j.cbpc.2010.08.002.
633 Knoepfel T, Himmerkus N, Guenzel D, Bleich M, Hernando N, Wagner CA (2019)
634 Paracellular transport of phosphate along the intestine. Am. J. Physiol.
635 Gastrointest. Liver Physiol. 317(2):G233–G241.
636 https://doi.org/10.1152/ajpgi.00032.2019.
637 Lefaix JL, Delanian S, Leplat JJ, Tricaud Y, Martin M, Nimrod A et al (1996) Successful
638 treatment of radiation-induced fibrosis using Cu/Zn-SOD and Mn-SOD: an
639 experimental study. Int. J. Radiat. Oncol. Biol. Phys. 35(2):305–312.
640 https://doi.org/10.1016/0360-3016(96)00061-2.
641 Lewin WC, Kamjunke N, Mehner T (2003) Phosphorus uptake by Microcystis during
642 passage through fish guts. Limnol. Oceanogr. 48(6):2392–2396.
643 https://doi.org/10.4319/lo.2003.48.6.2392.
644 Li CH, Sun HL, Chen AQ, Ning XX, Wu HF, Qin S et al (2010) Identification and
645 characterization of an intracellular Cu, Zn-superoxide dismutase (icCu/Zn-SOD)
646 gene from clam *Venerupis philippinarum*. Fish Shellfish Immunol. 28(3):499–
647 503. https://doi.org/10.1016/j.fsi.2009.11.021.
648 Li X, Wu LL, Zhou JL, Li YL, Qi T, Song XF et al (2025) Long-term phosphate
649 exposure effects on juvenile turbot (*Scophthalmus maximus*): Growth,
650 metabolism, and adaptive responses. Mar. Pollut. Bull. 213:117618.
651 https://doi.org/10.1016/j.marpolbul.2025.117618.
652 Liu JY, Ai TX, Yang J, Shang MJ, Jiang KJ, Yin Y et al (2024) Effects of salinity on
653 growth, digestive enzyme activity, and antioxidant capacity of spotbanded scat
654 (*Selenotoca multifasciata*) juveniles. Fishes 9(8):309.

https://doi.org/10.3390/fishes9080309.
Liu YT, Wang HM, Wu LF, Han J, Sui BY, Meng LN et al (2022) Intestinal changes associated with nitrite exposure in *Bufo gargarizans* larvae: Histological damage, immune response, and microbiota dysbiosis. Aquat. Toxicol. 249:106228. https://doi.org/10.1016/j.aquatox.2022.106228.
Livak KJ, Schmittgen TD (2001) Analysis of relative gene expression data using real-time quantitative PCR and the $2^{-\Delta\Delta CT}$ method. Methods 25(4):402–408. https://doi.org/10.1006/meth.2001.1262.
Lushchak VI (2016) Contaminant-induced oxidative stress in fish: a mechanistic approach. Fish Physiol. Biochem. 42(2):711–747. https://doi.org/10.1007/s10695-015-0171-5.
Menon SV, Kumar A, Middha SK, Paital B, Mathur S, Johnson R et al (2023) Water physicochemical factors and oxidative stress physiology in fish, a review. Front. Environ. Sci. 11:1240813. https://doi.org/10.3389/fenvs.2023.1240813.
Mereish KA, Solow R (1990) Effect of antihepatotoxic agents against microcystin-LR toxicity in cultured rat hepatocytes. Pharm. Res. 7(3):256. https://doi.org/10.1023/a:1015822028414.
Morrison M, Pope PB, Denman SE, McSweeney CS (2009) Plant biomass degradation by gut microbiomes: more of the same or something new? Curr. Opin. Biotechnol. 20(3):358–363. https://doi.org/10.1016/j.copbio.2009.05.004.
Muniz P, da Silva DAM, Bícego MC, Bromberg S, Pires-Vanin AMS (2015) Sewage contamination in a tropical coastal area (São Sebastião Channel, SP, Brazil). Mar. Pollut. Bull. 99(1-2):292–300. https://doi.org/10.1016/j.marpolbul.2015.07.046.
Mustafa SA, Al-Rudainy AJ, Salman NM (2024) Effect of environmental pollutants on fish health: An overview. Egypt. J. Aquat. Res. 50(2):225–233. https://doi.org/10.1016/j.ejar.2024.02.006.
Zimmer KD, Herwig BR, Laurich LM (2006) Nutrient excretion by fish in wetland ecosystems and its potential to support algal production. Limnol. Oceanogr. 51(1):197–207. https://doi.org/10.4319/lo.2006.51.1.0197.
Oberley LW, Buettner GR (1979) Role of superoxide dismutase in cancer: a review. Cancer Res. 39(4):1141–1149.
Padmini E (2010) Physiological adaptations of stressed fish to polluted environments: Role of heat shock proteins. In: Whitacre, D.M. (Ed.), Reviews of Environmental Contamination and Toxicology, vol 206, pp 1–27. https://doi.org/10.1007/978-1-4419-6260-7_1.
Qi T, Wu LL, Yu JC, Song ZC, Liu F, Li J et al (2023) Acute low-dose phosphate disrupts glycerophospholipid metabolism and induces stress in juvenile turbot (*Scophthalmus maximus*). Sci. Total Environ. 861:160430. https://doi.org/10.1016/j.scitotenv.2022.160430.
Qiao RX, Sheng C, Lu YF, Zhang Y, Ren HQ, Lemos B (2019) Microplastics induce intestinal inflammation, oxidative stress, and disorders of metabolome and microbiome in zebrafish. Sci. Total Environ. 662:246–253. https://doi.org/10.1016/j.scitotenv.2019.01.245.

699 Romano N, Zeng CS (2009) Evaluating the newly proposed protocol of incorporated
700 potassium in nitrate toxicity experiments at different salinities: A case study
701 with the tiger prawn, *Penaeus monodon*, juveniles. Aquaculture 289(3-4):304–
702 309. https://doi.org/10.1016/j.aquaculture.2009.01.035.
703 Rymuszka A, Sieroslawska A, Bownik A, Skowronski T (2007) In vitro effects of pure
704 microcystin-LR on the lymphocyte proliferation in rainbow trout
705 (*Oncorhynchus mykiss*). Fish Shellfish Immunol. 22(3):289–292.
706 https://doi.org/10.1016/j.fsi.2006.06.002
707 Selye H (1950) Stress and the general adaptation syndrome. Br. Med. J. 1 (4667):1383–
708 1392. https://doi.org/10.1136/bmj.1.4667.1383.
709 Shui Y, Guan ZB, Liu GF, Fan LM (2020) Gut microbiota of red swamp crayfish
710 *Procambarus clarkii* in integrated crayfish-rice cultivation model. AMB
711 Express 10(1):5. https://doi.org/10.1186/s13568-019-0944-9.
712 Slaoui M, Fiette L (2011) Histopathology procedures: from tissue sampling to
713 histopathological evaluation. Methods Mol. Biol. 691:69–82.
714 https://doi.org/10.1007/978-1-60761-849-2_4.
715 Soler P, Faria M, Barata C, García-Galea E, Lorente B, Vinyoles D (2021) Improving
716 water quality does not guarantee fish health: Effects of ammonia pollution on
717 the behaviour of wild-caught pre-exposed fish. PLoS One 16(8):e0243404.
718 https://doi.org/10.1371/journal.pone.0243404.
719 Sugiura SH (2024) Digestion and absorption of dietary phosphorus in fish. Fishes
720 9(8):324. https://doi.org/10.3390/fishes9080324.
721 Sugiura SH, Ferraris RP (2004) Contributions of different NaPi cotransporter isoforms
722 to dietary regulation of P transport in the pyloric caeca and intestine of rainbow
723 trout. J. Exp. Biol. 207(12):2055–2064. https://doi.org/10.1242/jeb.00971.
724 Tacon AGJ, Coelho RTI, Levy J, Machado TM, Neiva CRP, Lemos D (2023) Annotated
725 bibliography of selected papers dealing with the health benefits and risks of fish
726 and seafood consumption. Rev. Fish. Sci. Aquac.:2238821.
727 https://doi.org/10.1080/23308249.2023.2238821.
728 Thannickal VJ, Fanburg BL (2000) Reactive oxygen species in cell signaling. Am. J.
729 Physiol. Lung Cell. Mol. Physiol. 279(6):L1005–L1028.
730 https://doi.org/10.1152/ajplung.2000.279.6.L1005.
731 Toor HS, Sehgal HS, Brar CS (1983) Water-soluble phosphates: Observed effects on
732 embryonic development, hatching time, and survival of common carp. Trans.
733 Am. Fish. Soc. 45(2):134–135. https://doi.org/10.1577/1548-
734 8659(1983)45[134:WP]2.0.CO;2.
735 Ufodike E, Onusiriuka BJ (1990) Acute toxicity of inorganic fertilizers to African
736 catfish, *Clarias gariepinus* (Teugals). Aquac. Res. 21(2):181–186.
737 https://doi.org/10.1111/j.1365-2109.1990.tb00455.x.
738 Uruno A, Motohashi H (2011) The Keap1-Nrf2 system as an in vivo sensor for
739 electrophiles. Nitric Oxide 25(2):153–160.
740 https://doi.org/10.1016/j.niox.2011.02.007.
741 van Bussel CGJ, Mahlmann L, Kroeckel S, Schroeder JP, Schulz C (2013) The effect
742 of high ortho-phosphate water levels on growth, feed intake, nutrient utilization

and health status of juvenile turbot (*Psetta maxima*) reared in intensive recirculating aquaculture systems (RAS). Aquac. Eng. 57:63–70. https://doi.org/10.1016/j.aquaeng.2013.08.003.

Wang Y, Wang JW, Wu X, Zhao R, Zhang ZQ, Zhu JJ et al (2023) Synergetic effect and mechanism of elementary sulphur, $MgSO_4$ and KH_2PO_4 progressive reinforcement on pig manure composting nitrogen retention. Environ. Pollut. 331:121934. https://doi.org/10.1016/j.envpol.2023.121934.

Wang Y, Yang J, Yi J (2012) Redox sensing by proteins: Oxidative modifications on cysteines and the consequent events. Antioxid. Redox Signal. 16(7):649–657. https://doi.org/10.1089/ars.2011.4313.

Wu L, Li X, Zhou J, Qi T, Li Y, Song X et al (2025) Phosphate perils in marine aquaculture: Systematic toxicity assessment in turbot juveniles in cultivation. J. Environ. Sci. 156:619–631. https://doi.org/10.1016/j.jes.2024.10.005.

Yan X, Qi P, Guo B, Li J (2021) The advances in research of Nrf2 pathway involved in oxidative stress regulation in aquatic animals. Oceanol. Limnol. Sin. 52:799–812. https://doi.org/10.11693/hyhz20201100316.

Yu JC, Wang YF, Xiao YS, Li X, Xu XJ, Zhao HX et al (2021) Effects of chronic nitrate exposure on the intestinal morphology, immune status, barrier function, and microbiota of juvenile turbot (*Scophthalmus maximus*). Ecotoxicol. Environ. Saf. 207:111287. https://doi.org/10.1016/j.ecoenv.2020.111287.

Yu LL, Xiao MF, Tian FW, Chen W, Zhai QX (2024) Glycan utilization properties govern the cross-feeding network in gut microbiota: A focus on Bifidobacteria. Sci. Bull. 69(3):299–302. https://doi.org/10.1016/j.scib.2023.11.060.

Zengler K, Zaramela LS (2018) The social network of microorganisms - how auxotrophies shape complex communities. Nat. Rev. Microbiol. 16(6):383–390. https://doi.org/10.1038/s41579-018-0004-5.

Zhang JY, Zhang HJ, Chen YX (2006) Sensitive apoptosis induced by microcystins in the crucian carp (*Carassius auratus*) lymphocytes in vitro. Toxicol. In Vitro 20(5):560–566. https://doi.org/10.1016/j.tiv.2005.09.013.

Zhang SY, Li G, Wu HB, Liu XG, Yao YH, Tao L, Liu H (2011) An integrated recirculating aquaculture system (RAS) for land-based fish farming: The effects on water quality and fish production. Aquac. Eng. 45(3):93–102. https://doi.org/10.1016/j.aquaeng.2011.08.001.

Zong H, Yuan X, Wang L, Yu L, Hu Y, Huo C, Zhang Z (2017) Preliminary evaluation on the nitrogen and phosphorus loads by mariculture in China. Mar. Environ. Sci. 36(3):336–342. https://doi.org/10.13634/j.cnki.mes.2017.03.003.

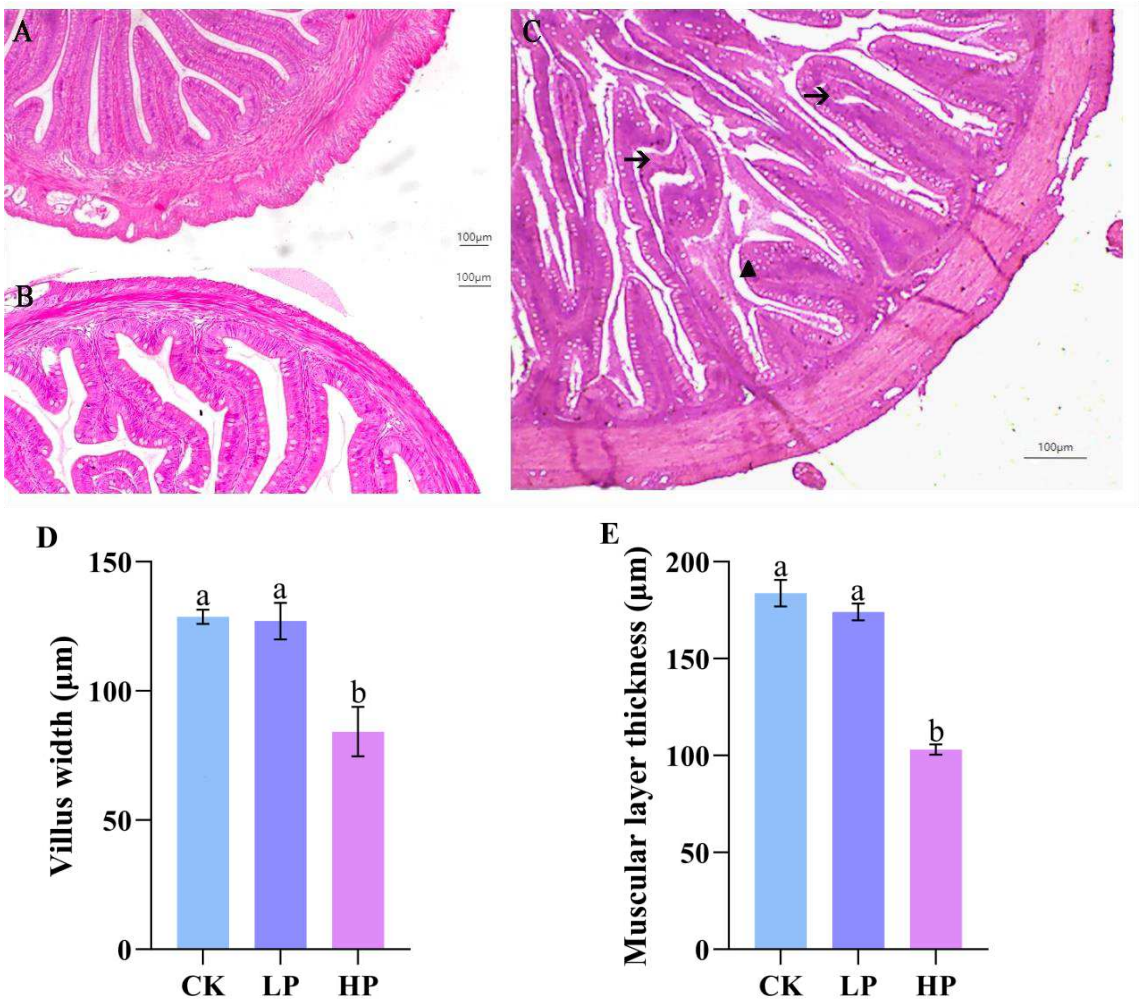

Fig. 1 Effects of different PO_4^{3-}-P concentrations on intestinal histology of juvenile turbot (A, B, C; Scale bar = 100 μm). (A) CK group (0 mg/L); (B) LP group (60 mg/L); (C) HP group (120 mg/L). Arrows indicate the presence of larger cavities within the intestinal villi; triangles signify pore formation in the epithelium of the intestinal villi. Quantitative morphometric analysis of intestinal histology (D, E). (D) Quantification of intestinal villus width (μm). (E) Quantification of intestinal muscularis thickness (μm). Data are presented as mean ± standard error (SE) (n = 3). Different letters indicate significant differences ($P < 0.05$).

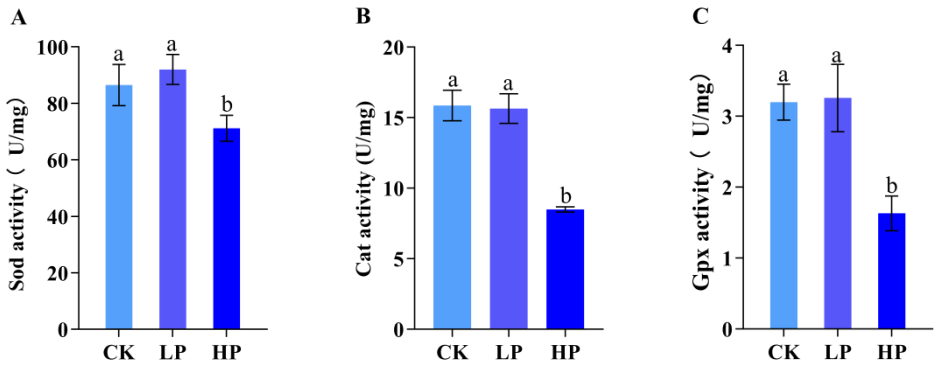

Fig. 2 Under different PO_4^{3-}-P concentrations (CK, LP, and HP), the oxidative stress enzyme activities in the turbot were represented by vertical bars as the mean ± standard error (SE) (n = 3).

Different letters indicate significant differences ($P < 0.05$).

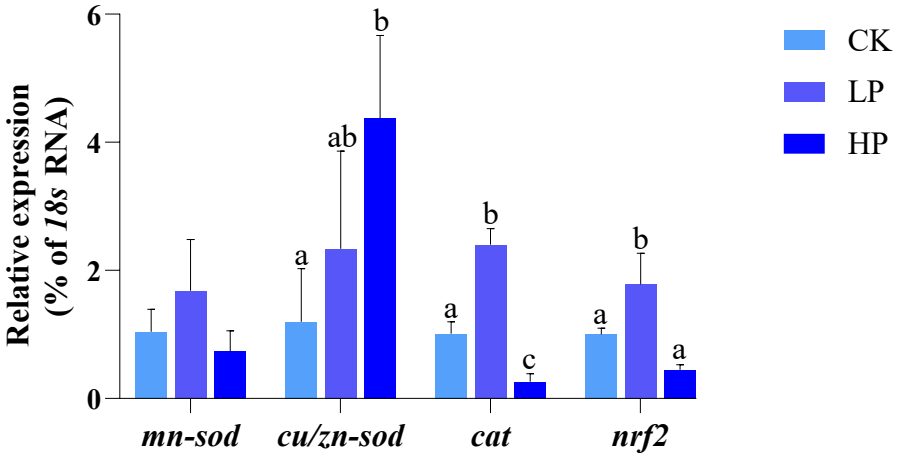

Fig. 3 The effects of different PO_4^{3-}-P concentrations (CK, LP, and HP) on the expression of key genes related to intestinal oxidative stress in juvenile turbot. The vertical bars represent the mean ± standard error (SE) (n = 3). Different letters indicate significant differences ($P < 0.05$).

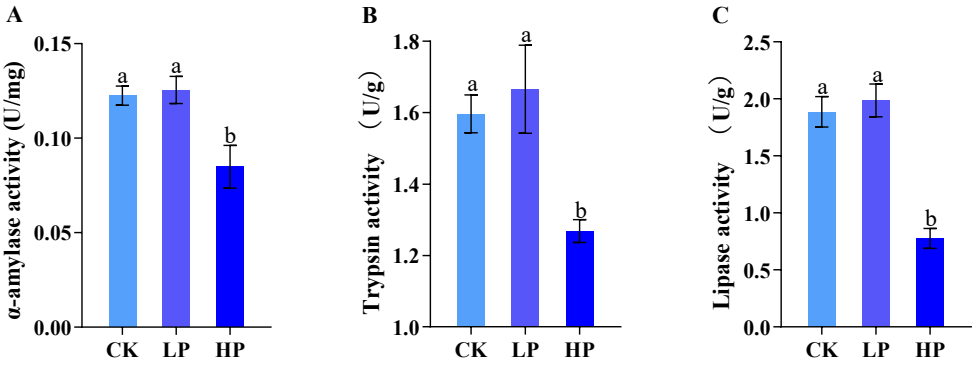

Fig. 4 Digestive enzyme activities in turbot under different PO_4^{3-}-P concentrations (CK, LP, HP), including α-amylase (A), trypsin (B), and lipase (C). Values represent the mean ± standard error (SE) (n = 3). Different letters indicate significant differences ($P < 0.05$).

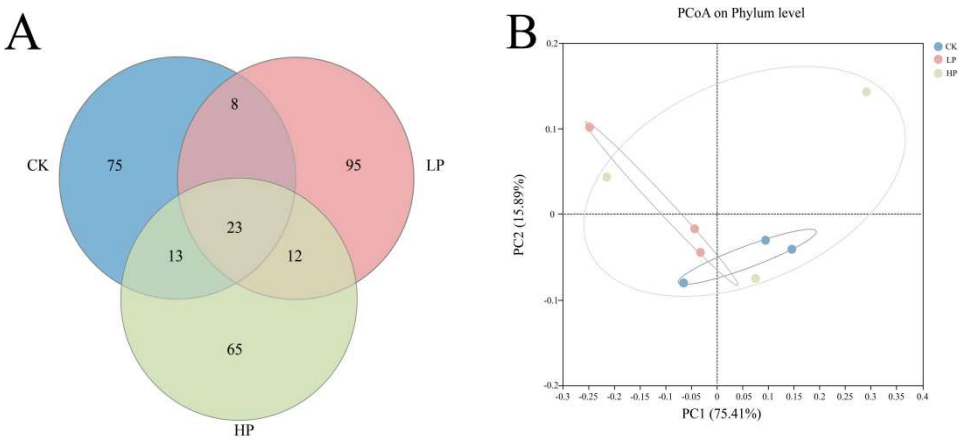

Fig. 5 Effects of PO_4^{3-}-P concentration on gut microbiota composition. (A) Venn diagram illustrating the number of shared and unique operational taxonomic units (OTUs) among different PO_4^{3-}-P treatment groups. (B) Principal coordinates analysis (PCoA) plot based on the Bray-Curtis distance metric, visualizing the dissimilarity of microbial community composition among samples. The blue, pink, and green colors indicate the CK, LP, and HP groups, respectively.

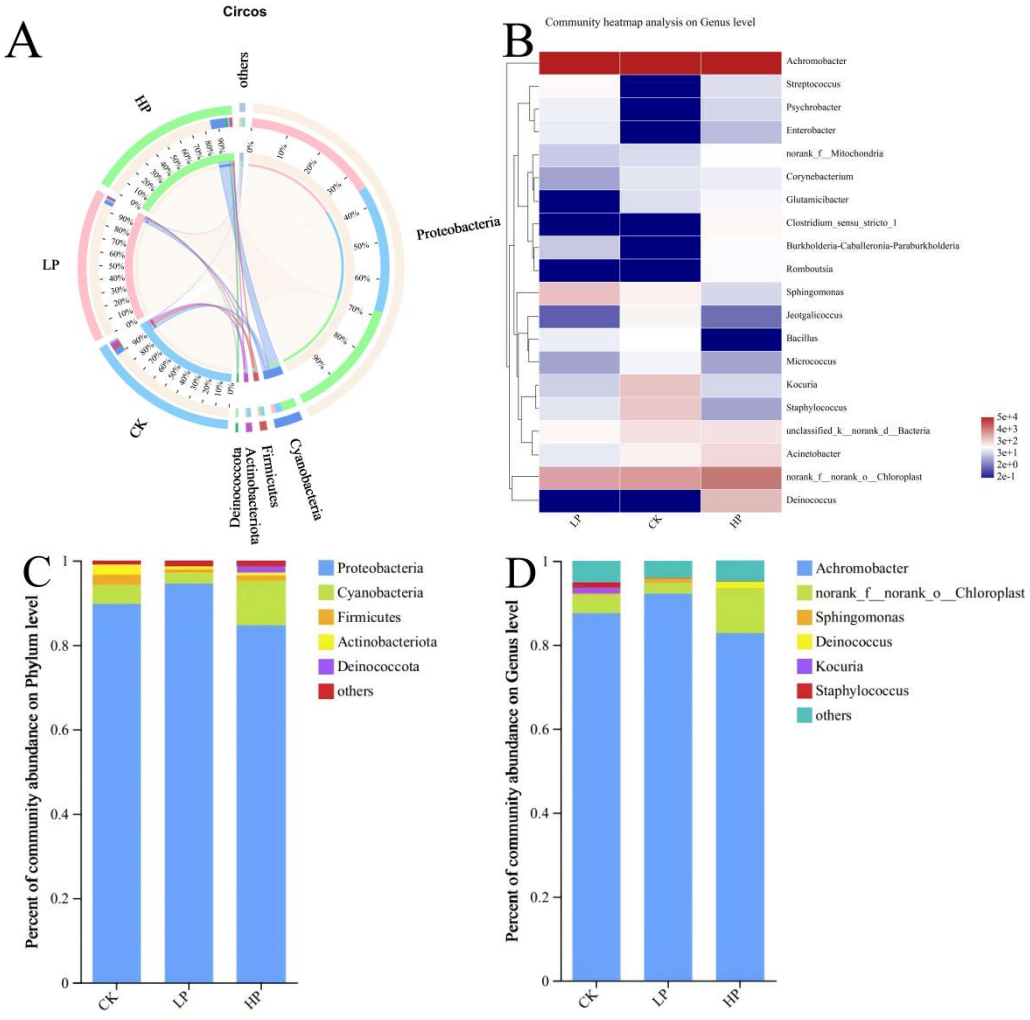

Fig. 6 Taxonomic classification and changes in the intestinal microbial composition of juvenile

turbot at different taxonomic levels. (A) Distribution of microbial communities at the phylum level. The circular diagram shows the dominant phyla in each group and the proportional distribution among different samples. (B) Heatmap analysis of the community at the genus level. The proportion of each genus is indicated by the color scale, with colors ranging from blue (low) to red (high). (C, D) Relative abundance of the intestinal microbiota at the phylum (C) and genus (D) levels using bar charts. The charts illustrate the composition of the top 5 most abundant taxa across all samples, categorizing those with low abundance as "others".

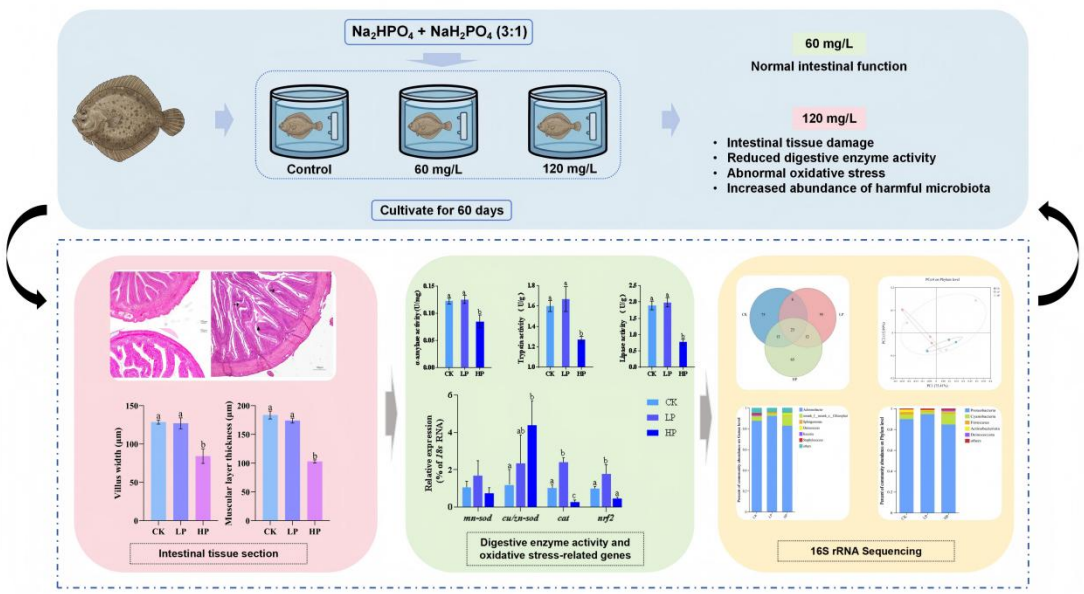

Fig. 7 Schematic diagram of the experimental design and effects of chronic PO_4^{3-}-P exposure (0, 60, and 120 mg/L for 60 days) on intestinal structure, digestive enzyme activity, oxidative stress, and intestinal microbiota of juvenile turbot.

Table 1

Primer sequence used in this study.

Primer name	Sequence (5′-3′)	Primer efficiency (%)
cu/zn-sod-F	TCACTTCAATCCCCATAGCA	106.7%
cu/zn-sod-R	CCGCAATCACATTCCCCAG	
mn-sod-F	TCTGAGGTTTAACGGGGGAG	102.5%
mn-sod-R	GGAGAGGGATGAGACCTGTTG	
cat-F	CAGTGCGGACGAAGATAA	96.6%
cat-R	CCTGGACGGCTGTAAACG	
nrf2-F	AATCTGCCCGTTGACGACTT	103.3%
nrf2-R	GGGCAGCCACTTTGTTCTTG	

18s-F	GGTCGGCGTCCAACTTCT	105.6%
18s-R	GGACATCTAAGGGCATCACAG	

820 **Table 2**

821 Alpha diversity indices of the intestinal microbiota treated with control (CK), low (LP), and high
822 (H) PO_4^{3-}-P concentrations.

Treatments	Shannon	Simpson	Chao	Ace
CK	0.6611±0.1193	0.7741±0.02619	55.83±18.51	52.76±13.92
LP	0.506±0.1677	0.8459±0.05624	55.67±19.4	55.39±18.99
HP	0.6692±0.1193	0.7196±0.02619	45.5±17.59	45.96±17.85

823